International Journal of Pharmaceutics 427 (2012) 358–364

Contents lists available at SciVerse ScienceDirect

International Journal of Pharmaceutics

journal homepage: www.elsevier.com/locate/ijpharm

Pharmaceutical Nanotechnology

Relationship between dissolution and bioavailability for nimodipine colloidal dispersions: The critical size in improving bioavailability

Qiang Fu[a], Longfa Kou[a], Cheng Gong[a], Mo Li[b], Jin Sun[a,*], Dong Zhang[a], Meina Liu[a], Xiaofan Sui[b], Kai Liu[c], Siling Wang[a], Zhonggui He[a,*]

[a] Department of Biopharmaceutics, School of Pharmacy, Shenyang Pharmaceutical University, Shenyang 110016, PR China
[b] Liaoning Institute for Food and Drug Control, Shenyang 110016, PR China
[c] Jiangsu Hengrui Medicine Co. Ltd., Lianyungang 222047, PR China

ARTICLE INFO

Article history:
Received 11 January 2012
Received in revised form 7 February 2012
Accepted 10 February 2012
Available online 19 February 2012

Keywords:
Nimodipine
Particle size
Dissolution
Bioavailability

ABSTRACT

To compare the dissolution and bioavailability for nimodipine microcrystals and nanocrystals, and to determine the critical size range in improving the oral absorption of nimodipine. Nimodipine microcrystals and nanocrystals were prepared using a microprecipitation method. The particle size was determined with a laser diffraction method. X-ray powder diffraction was applied to inspect the potential crystal form transition. The aqueous solubility was determined by shaking flasks, and the dissolution behavior was evaluated using the paddle method. The pharmacokinetics was performed in beagle dogs in a crossover experimental design. Three nimodipine colloidal dispersions (16296.7, 4060.0 and 833.3 nm) were prepared, respectively. Nimodipine had undergone crystal form transition during microprecipitation process, but experienced no conversion under the high-pressure homogenization. The colloidal dispersions did not show any difference in aqueous equilibrium solubility. Additionally, the three formulations also displayed similar dissolution curves in purified water and 0.05% SDS. The AUC for dispersions of 4060.0 and 833.3 nm sizes was 1.69 and 2.59-fold higher than that for 16296.7 nm system in dogs. To sum up, the critical particle size was found to be within the range of 833.3–4060.0 nm (average volume-weighted particle size) in improving the bioavailability of nimodipine, and dissolution performance was not an effective index in evaluating the bioavailability for nimodipine colloidal dispersions.

1. Introduction

It was estimated that about 40% of the new drug entities exhibited poor solubility, which hindered the bioavailability (Amidon et al., 1995). The poor solubility remained a major hurdle in the drug development and clinical use, and many drug candidates had to be abandoned despite favorable pharmacological activity (Wu and Benet, 2005). Therefore, it was necessary to develop an effective method to overcome the solubility-limitation and to improve the bioavailability.

Nowadays, reduction of particle size was a universal strategy for poorly soluble drugs in the pharmaceutical field (Kawabata et al., 2011). According to Ostwald Freundlich equation and Noyes–Whitney dissolution rate law, decreasing particle size to the micrometer scale (micronization) (Ning et al., 2011; Sigfridsson et al., 2009) or even to the nanometer scale (nanonization) (Shegokar and Müller, 2010; Van Eerdenbrugh et al., 2008; Sigfridsson et al., 2011) can lead to increased saturated solubility and dissolution rate, in turn, the bioavailability was improved. Moreover, it was believed that, within the certain size range, the smaller the particles, the higher the in vivo exposure. Recent investigations had confirmed this viewpoint with aprepitant (Wu et al., 2004), cilostazol (Jinno et al., 2006) and nitrendipine (Xia et al., 2010) as model drugs.

Interestingly, particle size-dependent absorption manner was also observed for itraconazole colloidal dispersions (Sun et al., 2011). Compared with the coarse dispersion, the AUC of 300 nm, 750 nm and 5.5 μm itraconazole dispersions was increased by 50.6, 43.9 and 6.5 times ($p < 0.05$), respectively. But it was worth to mention that the difference was not statistically significant ($p > 0.05$) in the AUC for nanocrystals of 300 and 750 nm, implying that the bioavailability could not be further enhanced with particle size reduction to a critical point (750 nm) or below. Thus, we proposed that there might be a critical particle size in improving the bioavailability of poorly soluble drugs. In addition, in our previous study, we found that two nimodipine nanocrystals (148 nm and 833 nm) were bioequivalent, demonstrating that bioavailability

* Corresponding authors at: Department of Biopharmaceutics, School of Pharmacy, Shenyang Pharmaceutical University, No. 59 Mailbox, No. 103 of Wenhua Road, Shenyang 110016, China. Tel.: +86 24 23986321; fax: +86 24 23986321.
E-mail addresses: sunjin66@21cn.com (J. Sun), hezhonggui@gmail.com, hezhonggui@vip.163.com (Z. He).

0378-5173/$ – see front matter © 2012 Elsevier B.V. All rights reserved.
doi:10.1016/j.ijpharm.2012.02.022

can be maximized by the preparation with the particle size of 833 nm and that particles smaller than the critical size were not necessary for further bioavailability improvement (Fu et al., under review). Accordingly, it is crucial to investigate if the bioavailability can remain constant for the preparations with larger particle size. Therefore, we would like to compare the in vivo performance of microcrystals and nanocrystals to evaluate the critical particle size in improving the bioavailability of nimodipine. Also in the same study (Fu et al., under review), although the 148 nm preparation was bioequivalent with 833 nm formulation, the 148 nm preparation showed a 3.42-fold increase in solubility, indicating that the aqueous solubility and dissolution rate were not "golden standard" in evaluating the quality of colloidal dispersions. Therefore, we would also like to investigate whether the dissolution could really reflect the in vivo performance of microcrystals and nanocrystals.

In this study, the nanocrystals and two microcrystals were prepared by a microprecipitation method, respectively. The relationship between dissolution and the pharmacokinetics was studied for the three colloidal dispersions. Finally, the critical particle size was developed, and whether dissolution could be an effective method in evaluating the quality of colloidal dispersions was discussed.

2. Methods

2.1. Materials

Nimodipine was purchased from Shanxi Ruicheng Pharm. Middle Product Co. Ltd. (Ruicheng, China). Lutrol® poloxamer 407 (F127) were kindly provided by BASF Co. Ltd. (Shanghai, China). Sodium deoxycholate was purchased from Beijing Aoboxing Biotech Co. Ltd. (Beijing, China). Hydroxypropyl methyl cellulose with a viscosity of 5 cps (HPMC-E5) was purchased from Huzhou Hopetop Pharm. Co. Ltd. (Huzhou, China). Sodium dodecyl sulphate (SDS), dimethyl sulfoxide (DMSO) and mannitol were purchased from Tianjin Bodi Chemical Holding Co. Ltd. (Tianjin, China). Maltose was purchased from Tianjin Kermel Chemical Reagent Co. Ltd. (Tianjin, China). Methanol, acetonitrile and *n*-hexane of chromatographic grade were purchased from Concord Technology Co. Ltd. (Tianjin, China). Deionized-distilled water was used throughout this study.

2.2. Preparation of the formulations

Generally, the colloidal dispersions were prepared by a microprecipitation method (or in combination with a high-pressure homogenization process), with the formula component fixed but process parameters (mixing temperature and homogenization pressure) varied, as shown in Table 1.

Microcrystals-1: The organic feeds were prepared by dissolving 700 mg of nimodipine and 100 mg of F127 in 1.5 mL of DMSO. Then the organic phase was injected instantaneously at a stirring rate of 15,000 rpm using FJ200 (Shanghai Specimen and Model Factory, Shanghai, China) into 100 mL of water phase equilibrated at 25 °C, which contained 700 mg of F127, 400 mg of HPMC-E5 and 100 mg of sodium deoxycholate.

Table 1
The key process parameters in preparation of the colloidal dispersions.

Formulations	Mixing zone temperatures (°C)	Homogenization pressure (bar) and cycle
Microcrystals-1	25	0
Microcrystals-2	3	0
Nanocrystals	3	1000 × 20

Microcrystals-2: The basic process was the same as microcrystals-1, but the water phase was equilibrated at 3 °C.

Nanocrystals: The nanocrystals were harvested following the homogenization of microcrystals-2 at 1000 bar for 20 cycles.

For convenient administration, the aqueous colloidal dispersions were freeze-dried using FDU-1100 (EYELA, Tokyo Rikakikai Co. Ltd., Japan) with 5% (w/v) maltose and 5% (w/v) mannitol as cryoprotectants. The freeze-drying processes were as follows: the samples were freezed at −70 °C in Sanyo V.I.P.® series −86 °C ultra-low-freezers (SANYO Electric Co. Ltd., Tokyo, Japan) for 6 h, and subsequently lyophilized at a temperature of −25 °C for 16 h, followed by a secondary drying phase of 2 h at 20 °C.

2.3. Characterization of the formulations

2.3.1. Particle size determination

Particle sizes were determined using the laser diffraction (LD) method. Measurements were performed with polarization intensity differential scattering technology (PIDS) for nanocrystals and without for microcrystals. The run length was 90 s for the measurements with PIDS, and 60 s for measurements without PIDS. The obscuration was adjusted to 35–40% for the measurement of nanocrystals and to 8–10% for that of microcrystals. The particle size was volume-weighted and expressed as d_{10}, d_{50}, d_{90} and mean diameter (d_{10}, d_{50} and d_{90} indicated that 10%, 50% and 90% of the particles were below that corresponding size, respectively). All measurements were performed in triplicate.

2.3.2. Microscope observation

To confirm the differences of diameters for the crystals, the Motic DMBA 450 microscope (MoticChina Group Co. Ltd., Beijing, China) was used. The nanocrystals were investigated without being diluted using an oil immersion with 1000-fold magnification.

2.3.3. X-ray powder diffraction (XRPD)

Diffraction patterns were determined for raw nimodipine, blank excipients, physical mixtures and lyophilized powders of nimodipine colloidal dispersions (microcrystals-1, microcrystals-2 and nanocrystals) using a Bruker AXS D8 discover (Bruker AXS, Karlsruhe, Germany) with a Cu line as the source of radiation, respectively. Standard runs were performed over a 2θ range of 3–45° with 40 kV as voltage, 40 mA as current and 0.013°/min as scanning rate.

Furthermore, the crystalline degree of the colloidal dispersions was analyzed using the JADE XRPD pattern processing software (Materials Data, Inc., USA).

2.3.4. Aqueous solubility of the formulations

2.3.4.1. HPLC analysis of nimodipine. A HPLC method was used to determine the content of nimodipine and to evaluate the solubility and dissolution rates of the formulations. The HPLC system was equipped with an L-2130 pump (Hitachi High-Technologies Corp., Tokyo, Japan) with acetonitrile–water (70:30, v/v) as mobile phase, and the flow rate was set at 1.0 mL/min. An L-2400 ultraviolet absorbance detector (Hitachi High-Technologies Corp., Tokyo, Japan) was used and operated at 236 nm. 20 μL of the samples was injected into Diamonsil® ODS (5 μm, 200 mm × 4.6 mm) column (Dikma Technologies, Beijing, China) maintained at 30 °C. The retention time was 6.7 min.

2.3.4.2. Aqueous solubility of nimodipine nanocrystals. The solubility was determined by a shake-flask method. Briefly, excess of lyophilized powders was added in purified water, 0.05% SDS and 0.3% SDS. The suspensions were shaken at 37 °C for 72 h in the dark. Then, aliquots were withdrawn and filtered through a 0.10 μm ANOW® filter (Hangzhou Anow microfiltration Co., Ltd., Hangzhou,

Table 2
Particle sizes for the nimodipine formulations (data were expressed as mean ± S.D., $n = 3$).

Formulations	d_{10} (nm)	d_{50} (nm)	d_{90} (nm)	$d_{average}$ (nm)
Microcrystals-1	1346.7 ± 52.6	8262.7 ± 369.5	47446.7 ± 40.4	16296.7 ± 161.7
Microcrystals-2	740.3 ± 202.1	3106.0 ± 183.6	8660.7 ± 671.5	4060.0 ± 31.2
Nanocrystals	157.0 ± 6.1	631.0 ± 7.0	2040.3 ± 18.9	833.3 ± 20.6

China). 1 mL of the primary filtrate was discarded, and the subsequent filtrate was analyzed immediately by HPLC. Each sample was prepared in triplicate.

2.3.4.3. Dissolution evaluations of the formulations. Dissolution tests were carried out using the USP Apparatus 2 setup (ZRS-8G; TIANDA TIANFA Technology Co. Ltd., Tianjin, China) with a paddle speed of 50 rpm. 900 mL of water, 0.05% SDS and 0.3% SDS equilibrated at 37 °C were used as dissolution medium. Accurately weighed samples (equivalent to 30 mg of nimodipine) were filled into 00 # gelatin capsules, which were placed into sinkers for test. At predetermined time intervals, 10 mL of samples was withdrawn and immediately filtered through 0.10 μm ANOW® filters, and 10 mL of fresh medium was replaced. In order to prevent crystallizing out the drug at a relative low temperature, the continuous filtrates were mixed with equal volume of acetonitrile, and the mixtures were analyzed by the HPLC method above.

2.4. Pharmacokinetic study

The pharmacokinetics was studied in accordance with the Guide for the Care and Use of Laboratory Animals. Six male beagle dogs weighing 9–13 kg were used and divided into 3 groups randomly, and the study was carried out in a crossover experimental design with a washout period of one week. The dogs were fasted for about 12 h prior to experiments, and were given water freely. The preparations were administered orally at a single dose of 30 mg. 3.0 mL of blood samples was taken into a heparinized blood collection tube via a detaining needle at pre-dose, 0.17, 0.33, 0.67, 1.0, 1.5, 2.0, 3.0, 4.0, 6.0, 8.0, 10.0 and 12.0 h post-dose. Dogs were provided with a standard lunch 4 h after dosing. The plasma fraction was obtained by centrifuging the samples at 3500 × *g* for 5 min, and was stored at −20 °C until analysis.

The nimodipine concentrations in plasma were determined by a validated liquid chromatography–dual mass spectrometry (LC–MS/MS) method after liquid–liquid extraction by *n*-hexane and anhydrous ether (1:1, v/v) with nitrendipine as internal standard. The chromatographic separations were acquired on an ACQUITY UPLC™ system (Waters Corp., Milford, MA) and BEH C18 column (50 mm × 2.1 mm, 1.7 μm; Waters Corp.) with a mobile phase composed of 80% acetonitrile and 20% water containing 0.1%, v/v acetic acid). The compounds were analyzed by multiple reaction monitoring (MRM) of the transitions of m/z 418.9 → 343.2 for nimodipine and m/z 360.8 → 315.2 for nitrendipine, respectively.

The maximum plasma concentration of nimodipine (C_{max}) and the time to reach C_{max} (t_{max}) were read directly from the plasma concentration versus time data. The area under curve (AUC) was calculated using the linear trapezoidal rule up to the last data point. The elimination rate constant (k) was the slope of the terminal four points in plasma concentration–time curve, and the half life of the preparation ($t_{1/2}$) was calculated by 0.693/k. All values were expressed as their mean ± S.E. (standard error). The relative bioavailability values (F) were calculated using the following formula with microcrystals-1 as a reference:

$$F(\%) = \frac{AUC_{test}}{AUC_{reference}} \times 100$$

2.5. Statistical analysis

The in vitro values (particle sizes and aqueous solubility) were expressed as their mean ± S.D. (standard deviation), and in vivo values (pharmacokinetics parameters) as their mean ± S.E. (standard error). The statistical analysis was made using the *t*-test. The differences were considered significant at $p < 0.05$.

3. Results

3.1. Particle sizes of the dispersions

The colloidal dispersions with different sizes were successfully prepared, as shown in Table 2. Through adjustment of the process parameters, the average diameters of particles decreased from 16296.7 nm to 4060.0 nm and further to 833.3 nm. Although the d_{90} showed that some particles in the nanocrystals were in the microscopic range, the d_{90} of microcrystals-1 and microcrystals-2 was 4.25 and 23.26-fold larger, respectively.

The microscope was used to examine the large particles in the three dispersions and to verify the measurement results from LD. As shown in Fig. 1, there were distinct differences in particle sizes among the three dispersions, in an agreement with the LD results. Only a small fraction of microcrystals could be detected in the nanocrystal dispersion, but more and larger particles in the microdispersions.

3.2. Crystal form of the colloidal dispersions

XRPD was used to evaluate the crystal form and potential polymorphic conversion during the preparing process. The XRPD patterns of crude nimodipine, blank excipients, physical mixtures and nimodipine colloidal dispersions are presented in Fig. 2. The characteristic peaks of crude nimodipine (at 2θ of 6.473° and 12.812°) were maintained in the profile of physical mixtures (Grunenberg et al., 1995; Cardoso et al., 2005), but disappeared in the colloidal dispersions. Moreover, a new peak centered on 2θ of 9.180° was observed in the microcrystals-1, microcrystals-2 and nanocrystals, demonstrating nimodipine had undergone a polymorphism transition from a stable crystal form to a metastable one during the microprecipitation process. Further calculation indicated that the crystalline degree of the microcrystals-1, microcrystals-2 and nanocrystals were 69.90 ± 8.81%, 65.63 ± 3.32% and 61.83 ± 6.70%, respectively.

3.3. Aqueous solubility study

3.3.1. Aqueous solubility of the three dispersions

Table 3 shows the equilibrium solubility of the three colloidal dispersions. For microcrystals-1, the solubility was about 8.15 ± 0.28 μg/mL in purified water and 8.31 ± 0.13 μg/mL in 0.05% SDS. But the solubility remained constant ($p > 0.05$) for the dispersions with varying particle size, regardless of the media used. It was inconsistent with the conventional Ostwald Freundlich equation.

3.3.2. Dissolution for the three colloidal dispersions

The in vitro dissolution curves for nimodipine colloidal dispersions are shown in Fig. 3. The three formulations displayed the

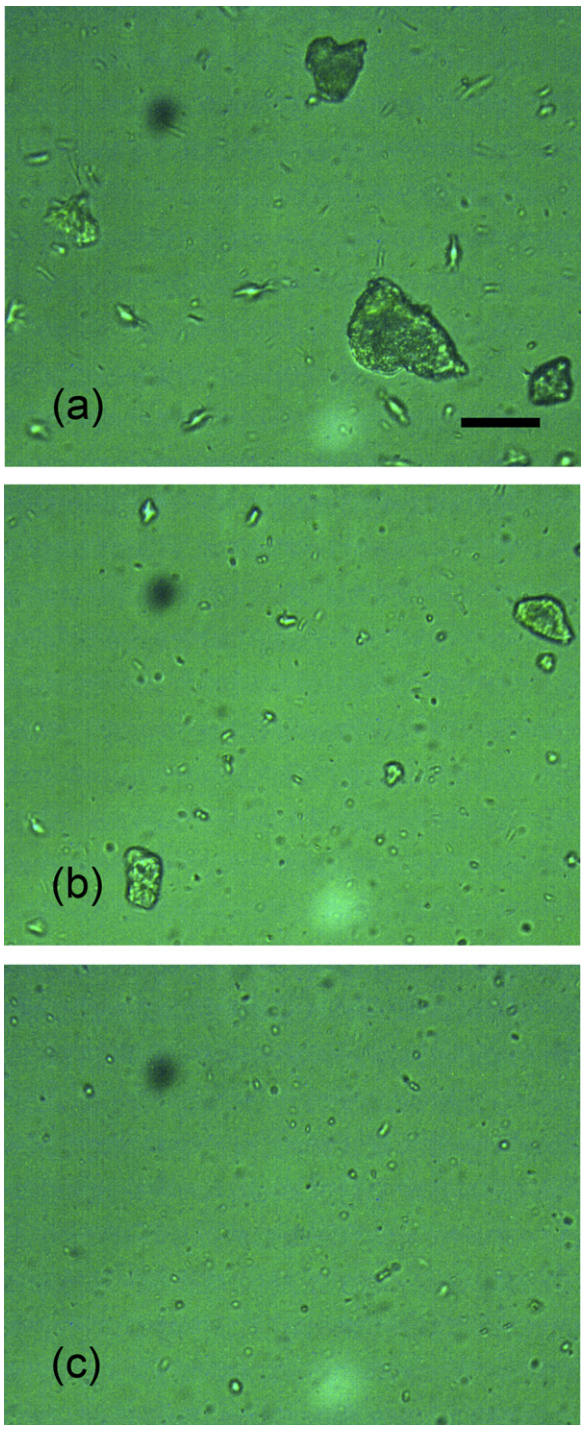

Fig. 1. Microscopes for the three nimodipine colloidal dispersions. (a) Nimodipine microcrystals-1; (b) nimodipine microcrystals-2; (c) nimodipine nanocrystals. The scale bar represents for 10 μm.

Table 3
Aqueous solubility for the nimodipine colloidal dispersions at 37 °C (data were expressed as mean ± S.D., $n = 3$).

Formulations	Aqueous solubility (μg/mL)	
	Water	0.05% SDS
Microcrystals-1	8.15 ± 0.28	8.31 ± 0.13
Microcrystals-2	7.48 ± 0.03	7.48 ± 0.05
Nanocrystals	6.99 ± 0.84	7.47 ± 0.64

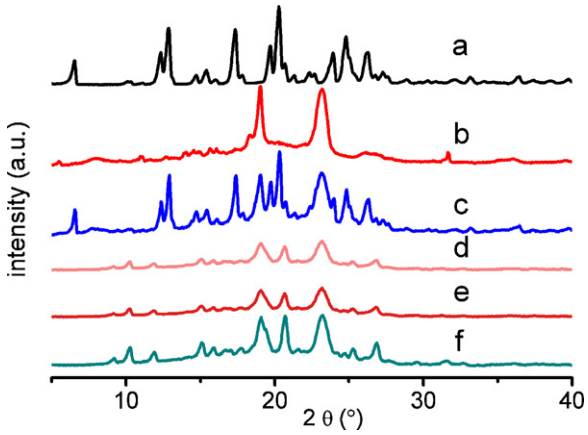

Fig. 2. XRPD patterns for (a) crude nimodipine, (b) blank excipients, (c) physical mixtures, (d) nimodipine microcrystals-1, (e) nimodipine microcrystals-2 and (f) nimodipine nanocrystals.

similar profiles in purified water, and the equilibrium (released about 6.11 ± 0.22% of total drugs) was reached at 20 min (Fig. 3b). As with 0.05% SDS, no significant difference was observed for the three preparations (Fig. 3a).

3.4. Pharmacokinetics

The plasma concentration–time curves and the pharmacokinetic parameters are shown in Fig. 4 and Table 4, respectively. The C_{max} and the AUC were significantly increased ($p < 0.05$) with particle size reduced. The C_{max} was increased from 142.35 ng mL^{-1} for microcrystals-1 to 234.16 ng mL^{-1} for microcrystals-2 and

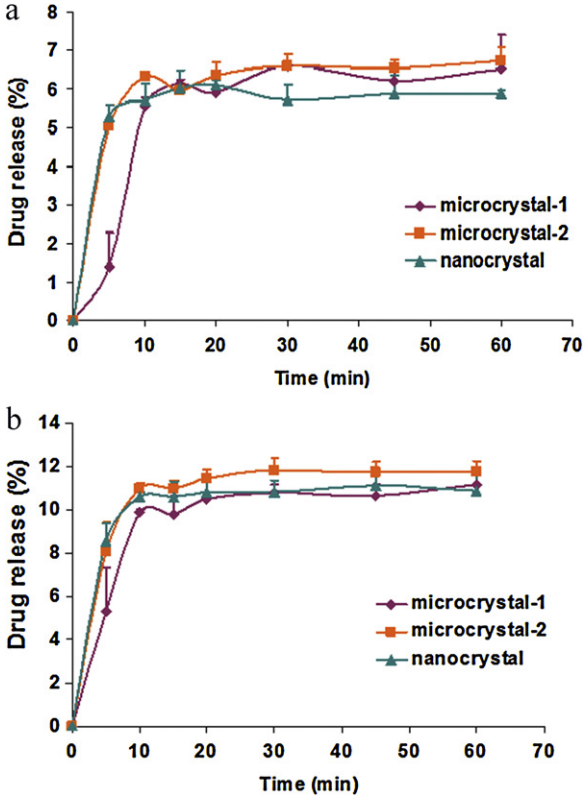

Fig. 3. Dissolution profiles for nimodipine microcrystals-1 (lavender color), microcrystals-2 (orange color) and nanocrystals (blue color) in purified water (a) and 0.05% SDS (b) (data are mean ± S.D., $n = 3$). (For interpretation of the references to color in this figure legend, the reader is referred to the web version of the article.)

Table 4
Pharmacokinetic parameters following oral administration of nimodipine colloidal dispersions (data were expressed as mean ± S.E., $n = 6$).

Parameters	Microcrystals-1	Microcrystals-2	Nanocrystals
C_{max} (ng mL^{-1})	142.35 ± 33.97	234.16 ± 42.68*	492.26 ± 152.40*,▲
t_{max} (min)	50.00 ± 4.47	55.00 ± 9.57	65.00 ± 11.88,
$t_{1/2}$ (min)	1.93 ± 0.14	1.69 ± 0.25	1.86 ± 0.19
k (min^{-1})	0.37 ± 0.03	0.46 ± 0.08	0.39 ± 0.05
AUC (ng min mL^{-1})	16558.08 ± 1875.82	25577.13 ± 2375.18*	61381.97 ± 15724.05*,▲
F	100.00%	154.47%	370.71%

* $p < 0.05$ versus microcrystals-1 as controls.
▲ $p < 0.05$ vesrsus microcrystals-2 as controls.

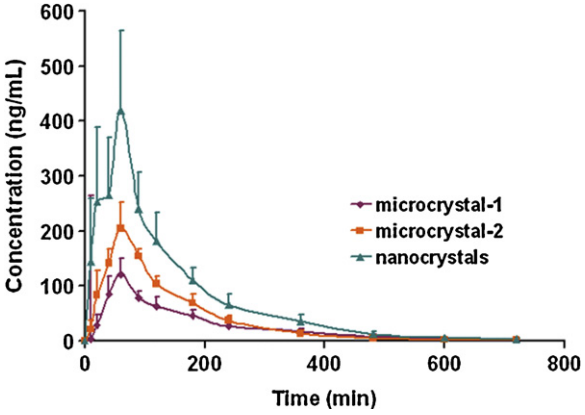

Fig. 4. Plasma concentration–time curves for the three nimodipine colloidal dispersions following oral administrations of 30 mg of nimodipine in beagle dogs (data are mean ± S.E., $n = 6$).

finally to 492.26 ng mL^{-1} for nanocrystals. The bioavailability of the nanocrystals was about 1.54 and 3.71-fold larger than that of microcrystals-1 and microcrystals-2, respectively. The t_{max} was delayed for nanocrystals to some extent, but it was necessary to point out that the difference was not statistically significant ($p > 0.05$) due to the discrete data and relative high SD. Also no statistically significant difference ($p > 0.05$) was found in $t_{1/2}$ and k among the three formulations.

4. Discussion

4.1. Preparation and characterization of the colloidal dispersions

4.1.1. Preparation of the colloidal dispersions

The particle size was decreased by lowering the microprecipitation temperature. Similar results had been reported previously. The temperature influenced the sizes in two ways. For one thing, the lowered temperature can lead to solubility decrease and further to supersaturation increase. Thus, the nucleating rate (Eq. (1)) was elevated and the number of crystal nucleus was increased correspondingly (Matteucci et al., 2006). Therefore, the particle size was decreased. For another, microprecipitation performed at a low temperature can inhibit the molecular diffusion and the subsequent Ostwald ripening.

$$B_0 = C \exp\left\{\frac{-16\pi\gamma^3 V_m N_A}{3(RT)^3[\ln(S)]^2}\right\} \quad (1)$$

where B_0 is the nucleation rate, S is the degree of supersaturation, γ is the interfacial tension, V_m is the molar volume, N_A is Avogadro's constant, R is the ideal gas constant and T is the microprecipitation temperature.

4.1.2. Crystal transformation

Undoubtedly, nimodipine had undergone crystal transition during microprecipitation (Fig. 2), because microprecipitation was truly a recrystallization process. Further XRPD calculation demonstrated that the crystal form and crystalline degree were not changed by varying the incubation temperature or passing through the high-pressure homogenizer. It was in an agreement with the previous report that the nanonization process could not affect the inner crystal structure of a model drug obviously (Gao et al., 2007).

4.2. Defects in the previously reported comparative study for microcrystals and nanocrystals

It is necessary to fix other influential factors (formulation components, preparation processes and crystal forms) when investigating the effects of crystal sizes on bioavailability. But more than one variable was always found in the previous studies. Firstly, the excipients were not kept the same (Sigfridsson et al., 2011; Wu et al., 2004). The amount of polymers or surfactants in nanocrystals was always larger than that in microcrystals. What is more, surfactants, such as SDS that could open the tight junctions of cells, were often used in nanocrystals, but not in microcrystals. Secondly, the microcrystals were always prepared by hammer milling, jet milling or ultrasonic treatment simply, inconsistent with the preparation process of nanocrystals (Wu et al., 2004; Jinno et al., 2006). Moreover, the micronized powders obtained by harsh milling treatment of the crude drugs will have increased tendency for electrostatic interaction, which could make the microcrystals agglomerate into larger ones and further block the oral absorption in vivo (Liversidge and Cundy, 1995; Perrut et al., 2005). Thirdly, the crystal form was sometimes different. The nanocrystals were always in the metastable state with higher solubility, while microcrystals or coarse powders in the stable form with lower solubility.

In this study, we had maintained these factors constant as possible. Therefore, the effects of particle sizes on in vitro evaluations and in vivo performances were investigated more objectively, excluding other factors, such as formulation composition, preparation process and crystal form transition.

4.3. Aqueous solubility and bioavailability of the colloidal dispersions

4.3.1. In vitro dissolution method was not an evaluation index for colloidal dispersions

The in vivo condition was supersaturation dissolution following 30 mg of nimodipine oral administration to beagle dogs (Fu et al., under review). Moreover, the importance of dissolution under non-sink condition had been stressed previously (He et al., 2004), because it could distinguish tiny differences in the quality of formulations. But for the three dispersions, significant difference could be tested neither in purified water, nor in 0.05% SDS, suggestive of the similar in vivo dissolution performance.

Although the in vitro supersaturation dissolution did not discriminate the differences, the in vivo pharmacokinetic study had

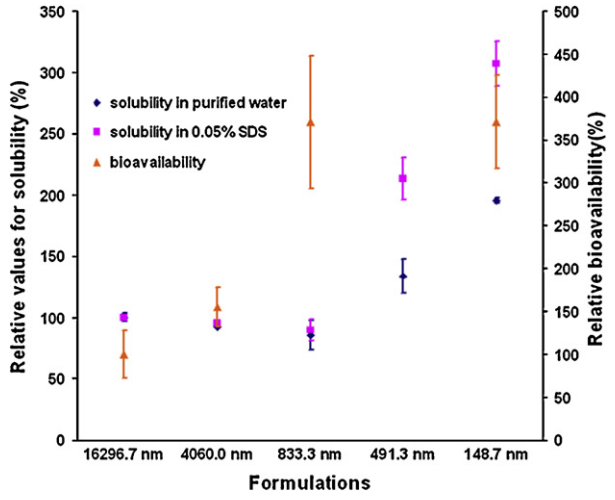

Fig. 5. Relative values of the solubility (in purified water and 0.05% SDS) and relative bioavailability for the dispersions with sizes of 4060.0, 833.3, 491.3 and 148.7 nm, with 16296.7 nm formulation as a reference (data are mean ± S.E.).

tested the differences among the three preparations. It was clear that the reduction of particle size leads to improvements in oral absorption of nimodipine, up to 1.54 and 3.71-fold increase in AUC ($p < 0.05$). Thus, the in vivo performance could not be correlated with the in vitro dissolution. In other words, the in vitro dissolution method was not an evaluation index for colloidal dispersions. The previous dissolution profile and pharmacokinetic study further confirmed this finding (Fu et al., under review).

4.3.2. Discrepancies in the trend of solubility and bioavailability

Generally, we could observe two different trends for aqueous solubility and bioavailability with particle size reduction, as shown in Fig. 5. In particular, the aqueous solubility remained constant with particle size reduction from 16296.7 nm to 833.3 nm, but then increased markedly for further reduction regardless of the medium. Instead, the bioavailability increased evidently for the initial decrease in particle sizes, but stayed constant for the subsequent decrease.

As we know, saturated solubility is a compound specific constant depending on the temperature and the aqueous medium. This is the reason why solubility was not increased despite the 19.6-fold reduction in particle size. But the Ostwald Freundlich equation could explain the subsequent increase in solubility by further downsizing the nanocrystals: with the particle size below 1 μm, decrease in size can improve the intrinsic solubility or saturated solubility (Patravale et al., 2004).

The discrepancy in the trends of solubility and bioavailability may result from the special membrane transporting mechanism of the nanocrystals, because solubility and permeability were two dominant factors affecting the oral bioavailability of a drug. In our previous study, we had found out that the nimodipine nanocrystals gained access into the mesenteric lymphatic systems by being taken up into enterocytes via macropinocytosis and caveolin-mediated endocytosis pathways. Moreover, some clues in this study could further confirm this finding: (1) as shown in Fig. 4, the error bars in the profile of nanocrystals were a bit larger than that of the microcrystals, and it could be attributed to the various expression levels for the proteins on the gut cell membranes of the six dogs (Bernatchez et al., 2011); (2) previous studies had demonstrated that a lag-time was prolonged and the absorption was delayed when drugs absorbed via lymphatic transport because of the initial hydrolysis of the triglycerides (Charman and Stella, 1986; Lind et al., 2008). In this study, the t_{max} was prolonged to some extent, although the differences were not statistically significant. In summary, the special mechanisms were probably involved in the absorption of nimodipine nanocrystals.

In addition, two review articles published recently emphasized the significance of particle size on the endocytosis of nanomedicines, and particles smaller than 1 μm could be internalized by macropinocytosis (Sahay et al., 2010; Roger et al., 2010). The variation in AUC (for microcrystals-1, microcrystals-2 and nanocrystals) was due to the particle size-dependent membrane transporting mechanism (avoiding first-pass metabolism). Further reduction of particle sizes to 148.7 nm did not show increasing linearity in the bioavailability due to the saturation for the proteins involved in the vesicle trafficking. Thus, a critical point of particle size-bioavailability was formed, namely the critical particle size in improving the bioavailability (Kaneniwa et al., 1978).

It is necessary to perform nanonization for drugs belonging to BCS II, at least for nimodipine. When the diameters come to the nanoscopic level, however, we need to redefine the critical particle size based on the pharmacokinetic properties of the colloidal dispersions, below which the bioavailability would not be improved.

5. Conclusions

In the present study, it was demonstrated that the in vivo exposure was improved by reducing the particle size to nanoscale. Thus, it is necessary to nanosize nimodipine, a poorly soluble drug. But the aqueous solubility and the supersaturation dissolution could not discriminate the difference in vitro, and dissolution was not an effective index in evaluating the bioavailability of colloidal dispersions, because special mechanisms were involved in the absorption of nimodipine nanocrystals, as previously investigated. Combining the above results, the critical particle size was ascertained to be within the range of 833.3–4060.0 nm (average volume-weighted particle size) in improving the bioavailability of nimodipine.

Acknowledgments

This work was financially supported from the National Nature Science Foundation of China (No. 81173008), from the National Basic Research Program of China (973 Program) No. 2009CB930300, from Project for Excellent Talents of Liaoning Province (No. LR20110028) and from Key Project for Drug Innovation of China (No. 2010ZX09401-304).

References

Amidon, G.L., Lennernäs, H., Shah, V.P., Crison, J.R., 1995. A theoretical basis for a biopharmaceutic drug classification: the correlation of in vitro drug product dissolution and in vivo bioavailability. Pharm. Res. 12, 413–420.

Bernatchez, P., Sharma, A., Bauer, P.M., Marin, E., Sessa, W.C., 2011. A noninhibitory mutant of the caveolin-1 scaffolding domain enhances eNOS-derived NO synthesis and vasodilation in mice. J. Clin. Invest. 121, 3747–3755.

Cardoso, T.M., Rodriguesm, P.O., Stulzer, H.K., Segatto Silva, M.A., do Rosário Matos, J., 2005. Physical–chemical characterization and polymorphism determination of two nimodipine samples deriving from distinct laboratories. Drug Dev. Ind. Pharm. 31, 631–637.

Charman, W.N.A., Stella, V.J., 1986. Effect of lipid class and lipid vehicle volume on the intestinal lymphatic transport of DDT. Int. J. Pharm. 33, 165–172.

Fu, Q., Sun, J., Ai, X., Kou, L., Gong, C., He, Z. What accounts for unfavoured in vitro in vivo correlation of nimodipine nanocrystals and solid dispersions: molecular form versus crystal form, under review.

Gao, L., Zhang, D., Chen, M., Zheng, T., Wang, S., 2007. Preparation and characterization of an oridonin nanosuspension for solubility and dissolution velocity enhancement. Drug Dev. Ind. Pharm. 33, 1332–1339.

Grunenberg, A., Keil, B., Henck, J.-O., 1995. Polymorphism in binary mixtures, as exemplified by nimodipine. Int. J. Pharm. 118, 11–21.

He, Z., Zhong, D., Chen, X., Liu, X., Tang, X., Zhao, L., 2004. Development of a dissolution medium for nimodipine tablets based on bioavailability evaluation. Eur. J. Pharm. Sci. 21, 487–491.

Jinno, J., Kamada, N., Miyake, M., Yamada, K., Mukai, T., Odomi, M., Toguchi, H., Liversidge, G.G., Higaki, K., Kimura, T., 2006. Effect of particle size reduction on

dissolution and oral absorption of a poorly water-soluble drug, cilostazol, in beagle dogs. J. Control. Release 111, 56–64.
Kaneniwa, N., Watari, N., Iijima, H., 1978. Dissolution of slightly soluble drugs. V. Effect of particle size on gastrointestinal drug absorption and its relation to solubility. Chem. Pharm. Bull. (Tokyo) 26, 2603–2614.
Kawabata, Y., Wada, K., Nakatani, M., Yamada, S., Onoue, S., 2011. Formulation design for poorly water-soluble drugs based on biopharmaceutics classification system: basic approaches and practical applications. Int. J. Pharm. 420, 1–10.
Lind, M.L., Jacobsen, J., Holm, R., Müllertz, A., 2008. Intestinal lymphatic transport of halofantrine in rats assessed using a chylomicron flow blocking approach: the influence of polysorbate 60 and 80. Eur. J. Pharm. Sci. 35, 211–218.
Liversidge, G.G., Cundy, K.C., 1995. Particle size reduction for improvement of oral bioavailability of hydrophobic drugs: I. Absolute oral bioavailability of nanocrystalline danazol in beagle dogs. Int. J. Pharm. 125, 91–97.
Matteucci, M.E., Hotze, M.A., Johnston, K.P., Williams, R.O., 2006. Drug nanoparticles by antisolvent precipitation: mixing energy versus surfactant stabilization. Langmuir 22, 8951–8959.
Ning, X., Sun, J., Han, X., Wu, Y., Yan, Z., Han, J., He, Z., 2011. Strategies to improve dissolution and oral absorption of glimepiride tablets: solid dispersion versus micronization techniques. Drug Dev. Ind. Pharm. 37, 727–736.
Patravale, V.B., Date, A.A., Kulkarni, R.M., 2004. Nanosuspensions: a promising drug delivery strategy. J. Pharm. Pharmacol. 56, 827–840.
Perrut, M., Jung, J., Leboeuf, F., 2005. Enhancement of dissolution rate of poorly-soluble active ingredients by supercritical fluid processes. Part I: Micronization of neat particles. Int. J. Pharm. 288, 3–10.
Roger, E., Lagarce, F., Garcion, E., Benoit, J.P., 2010. Biopharmaceutical parameters to consider in order to alter the fate of nanocarriers after oral delivery. Nanomedicine (Lond.) 5, 287–306.
Sahay, G., Alakhova, D.Y., Kabanov, A.V., 2010. Endocytosis of nanomedicines. J. Control. Release 145, 182–195.
Shegokar, R., Müller, R.H., 2010. Nanocrystals: industrially feasible multifunctional formulation technology for poorly soluble actives. Int. J. Pharm. 399, 129–139.
Sigfridsson, K., Lundqvist, A.J., Strimfors, M., 2009. Particle size reduction for improvement of oral absorption of the poorly soluble drug UG558 in rats during early development. Drug Dev. Ind. Pharm. 35, 1479–1486.
Sigfridsson, K., Nordmark, A., Theilig, S., Lindahl, A., 2011. A formulation comparison between micro- and nanosuspensions: the importance of particle size for absorption of a model compound, following repeated oral administration to rats during early development. Drug Dev. Ind. Pharm. 37, 185–192.
Sun, W., Mao, S., Shi, Y., Li, L.C., Fang, L., 2011. Nanonization of itraconazole by high pressure homogenization: stabilizer optimization and effect of particle size on oral absorption. J. Pharm. Sci. 100, 3365–3373.
Van Eerdenbrugh, B., Van den Mooter, G., Augustijns, P., 2008. Top-down production of drug nanocrystals: nanosuspension stabilization, miniaturization and transformation into solid products. Int. J. Pharm. 364, 64–75.
Wu, C.Y., Benet, L.Z., 2005. Predicting drug disposition via application of BCS: transport/absorption/elimination interplay and development of a biopharmaceutics drug disposition classification system. Pharm. Res. 22, 11–23.
Wu, Y., Loper, A., Landis, E., Hettrick, L., Novak, L., Lynn, K., Chen, C., Thompson, K., Higgins, R., Batra, U., Shelukar, S., Kwei, G., Storey, D., 2004. The role of biopharmaceutics in the development of a clinical nanoparticle formulation of MK-0869: a beagle dog model predicts improved bioavailability and diminished food effect on absorption in human. Int. J. Pharm. 285, 135–146.
Xia, D., Cui, F., Piao, H., Cun, D., Piao, H., Jiang, Y., Ouyang, M., Quan, P., 2010. Effect of crystal size on the in vitro dissolution and oral absorption of nitrendipine in rats. Pharm. Res. 27, 1965–1976.